Published in final edited form as:
Dev Biol. 2008 April 1; 316(1): 62–73. doi:10.1016/j.ydbio.2008.01.012.

A distinct cohort of progenitor cells participates in synovial joint and articular cartilage formation during mouse limb skeletogenesis

Eiki Koyama[a], **Yoshihiro Shibukawa**[b], **Motohiko Nagayama**[a], **Hiroki Sugito**[b], **Blanche Young**[a], **Takahito Yuasa**[a], **Takahiro Okabe**[a], **Takanaga Ochiai**[a], **Nobuhiko Kamiya**[c], **Ryan B. Rountree**[d,^], **David M. Kingsley**[d], **Masahiro Iwamoto**[a], **Motomi Enomoto-Iwamoto**[a], and **Maurizio Pacifici**[a]

a*Department of Orthopaedic Surgery, Thomas Jefferson University College of Medicine, Philadelphia, Pennsylvania 19107, USA*

b*Tokyo Dental College, Department of Periodontics, Tokyo, Japan*

c*Molecular developmental Biology Group, Laboratory of Reproductive and Developmental Toxicology, NIES, Research Triangle Park, NC 27709*

d*Department of Developmental Biology and HHMI, Stanford University School of Medicine, Stanford, California 94305, USA*

Abstract

The origin, roles and fate of progenitor cells forming synovial joints during limb skeletogenesis remain largely unclear. Here we produced prenatal and postnatal genetic cell fate-maps by mating ROSA-*LacZ*-reporter mice with mice expressing *Cre*-recombinase at prospective joint sites under the control of *Gdf5* regulatory sequences (*Gdf5-Cre*). Reporter-expressing cells initially constituted the interzone, a compact mesenchymal structure representing the first overt sign of joint formation, and displayed a gradient-like distribution along the ventral-to-dorsal axis. The cells expressed genes such as *Wnt9a, Erg* and *collagen IIA*, remained predominant in the joint-forming sites over time, gave rise to articular cartilage, synovial lining and other joint tissues, but contributed little if any to underlying growth plate cartilage and shaft. To study their developmental properties more directly, we isolated the joint-forming cells from prospective autopod joint sites using a novel microsurgical procedure and tested them in vitro. The cells displayed a propensity to undergo chondrogenesis that was enhanced by treatment with exogenous rGdf5 but blocked by *Wnt9a* over-expression. To test roles for such *Wnt*-mediated anti-chondrogenic capacity in vivo, we created conditional mutants deficient in Wnt/β-catenin signaling using *Col2-Cre* or *Gdf5-Cre*. Synovial joints did form in both mutants; however, the joints displayed a defective flat cell layer normally abutting the synovial cavity and expressed markedly reduced levels of *lubricin*. In sum, our data indicate that cells present at prospective joint sites and expressing *Gdf5* constitute a distinct cohort of progenitor cells responsible for limb joint formation. The cells appear to be patterned along specific limb symmetry axes and rely on local signaling tools to make distinct contributions to joint formation.

Correspondence to: Maurizio Pacifici maurizio.pacifici@jefferson.edu; or Motomi Enomoto-Iwamoto motomi.iwamoto@jefferson.edu.
^*Present address*: BN-Immunotherapeutics, 2425 Garcia Avenue, Mountain View, CA 94043

Keywords

Synovial joint formation; Interzone; Limb development; Articular cartilage; Gdf5; Wnt9a; Signaling pathways

Introduction

Synovial joints are essential for skeletal function and quality of life. As a result, joint biology has attracted extensive research activity for years and much has come to be understood about joint structure and organization and the biomechanical properties and roles of articular cartilage, ligaments, synovium, capsule and other components in join functioning and maintenance. There is also a considerable amount of information on joint susceptibility to malfunction during natural aging or conditions such as osteoarthritis that affect the vast majority of individuals over the age of sixty with costly and painful consequences (Bird, 2003; Brandt, 2004; Buckwalter et al., 2006). On the other hand, relatively little is known about how synovial joints actually come to acquire their structure, organization and function in the developing embryo and in particular what the nature of joint progenitor cells is and how the cells give rise to each joint component with its appropriate structural and functional characteristics and organization (Pacifici et al., 2005). Information at the cellular and molecular level in this area would be of fundamental interest and broad relevance; for instance, it could be used to prime stem cells with joint-specific regenerative or restorative capacity for future therapeutic applications.

In the embryonic limb, skeletogenesis initiates with formation of uninterrupted pre-chondrogenic cell condensations, including the Y-shaped condensation spanning the stylopod and zeugopod regions and the digital rays in the autopod region (Dangleish, 1964; Hamrick, 2001; Hinchliffe and Johnson, 1980). The first overt sign of joint formation is the emergence of a mesenchymal interzone at each prospective joint site (Holder, 1977; Mitrovic, 1978). The interzone is a tripartite tissue structure that displays a dense intermediate cell layer and two outer cell layers each facing the epiphyseal end of adjacent long bone anlagen. Microsurgical removal of the interzone region from prospective elbow site was originally found to lead to joint ablation and fusion of cartilaginous humerus with radius and ulna, suggesting that the region is essential for joint formation (Holder, 1977). Subsequent studies reinforced this idea and suggested that the interzone layers are largely responsible for development of articular chondrocytes (Bland and Ashhurst, 1996). Instead, ultrastructural analysis in developing rat embryos indicated that the outer interzone layers participate in initial lengthening of long bone anlagen by appositional growth, whereas articular chondrocytes would largely derive from the intermediate layer (Ito and Kida, 2000). Thus, despite wide recognition that the interzone region is essential for joint formation, the specific developmental roles, fate and mechanisms of action of its cells remain poorly understood (Pacifici et al., 2005).

Molecular and genetic studies have revealed more recently that nascent joints and interzone cells express a number of genes that include *Gdf5, Wnt9a, Wnt4, Gli3, CD44, Erg* and *Noggin* (Brunet et al., 1998; Hartmann and Tabin, 2001; Iwamoto et al., 2000; Storm et al., 1994). Gdf5 is a factor with chondrogenic activity, and congenital *Gdf5* mutations cause defects in digit, wrist and ankle joints in mouse and human (Storm et al., 1994; Thomas et al., 1997). Wnt9a and Noggin are factors with anti-chondrogenic activity. Experimental ablation of *Noggin* in mouse prevents limb joint formation and causes skeletal fusions (Brunet et al., 1998), and ablation of *Wnt9a* along with *Wnt4* disrupts joint formation and also causes some fusions (Spater et al., 2006b). One important and intriguing concept stemming from these and related studies is that interzone function and joint formation require the intervention of gene products with chondrogenic and anti-chondrogenic activities. The latter would be critical for

establishing and maintaining the initial mesenchymal character of cells present at joint sites, while the former would be needed for formation of articular cartilage and fibro-cartilaginous joint structures such as ligaments.

To tackle some of the above and related questions, we developed a system to carry out genetic cell fate map analysis of embryonic joint formation by mating ROSA-*LacZ* reporter mice (Soriano, 1999) with *Gdf5-Cre* transgenic mice (Rountree et al., 2004). Initial data revealed that the reporter-positive cells remained in the developing joint area and were present in the articular layers. Here, we extended this approach and carried out an in depth analysis of distribution, roles and fate of *Gdf5*-expressing reporter-positive cells at consecutive prenatal and postnatal stages. To test the properties of the joint-forming cells more directly, we also established a novel procedure for microsurgical isolation of interzone region and culturing of its cells, and tested endogenous differentiation capacity and modulation by exogenous rGdf5 protein or forced *Wnt9a* expression. Given that Wnt9a signals via β-catenin (Guo et al., 2004), we conditionally ablated β-*catenin* by *Gdf5-Cre* or *Col2-Cre* and carried out detailed analyses of resulting joint phenotypes. The results of the study shed new light on joint formation. In particular, they establish that the *Gdf5*-expressing cells give rise to most if not all joint tissues including articular cartilage, ligaments and inner synovial lining, but contribute negligibly to adjacent long bone cartilaginous shaft and growth plate formation. The cells thus appear to constitute a specialized and distinct cohort of limb skeletal progenitor cells devoted to joint formation.

Materials and methods

Mouse lines, mating and genotyping

Gdf-5-Cre transgenic mice were described previously (Rountree et al., 2004) and line B was used in the present study. Mice were mated with Rosa R26R Cre-inducible *LacZ* (β-galactosidase) mice in which the reporter β-galactosidase gene is silent and becomes irreversibly expressed after Cre-recombinase removal of a floxed silencer within its constitutive promoter reporter mice (Soriano, 1999). Mice conditionally deficient in *β-catenin* were created by mating *β-catenin* floxed mice (*β-catenin*$^{fl/fl}$) possessing loxP sites in introns 1 and 6 of the β-catenin gene (6.129-Ctnnb1tmKem/KnwJ line purchased from the Jackson Laboratory) with *Col2a1-Cre* mice (kindly provided by Dr. Y. Yamada, NIDCR) or *Gdf5-Cre* mice. Genotyping of β-*catenin* allele was carried out according to protocol from Jackson Laboratory. Two Wnt/β-catenin reporter transgenic mice were used. *TOPGAL* mice (Tg(Fos-lacZ)34Efu/J line) contain a *lacZ* gene under the control of regulatory sequences consisting of 3 consensus LEF/TCF-binding motifs upstream of a minimal *c-fos* promoter (DasGupta and Fuchs, 1999) and were purchased from the Jackson Laboratory. *BATLacz* mice express *lacZ* under the control of x8 LEF/TCF-binding sites and a minimal promoter from *Xenopus Siamosis* (Nakaya et al., 2005) and were kindly provided by Dr. T.E. Yamaguchi (National Cancer Institute at Frederick). Pregnant mice and postnatal mice were sacrificed by IACUC approved methods. Genotyping was carried out with DNA isolated from tail clips. Staining for β-galactosidase on whole embryos or limb sections was accomplished by standard protocols (Lobe et al., 1999).

In situ hybridization

This procedure was carried out as described previously (Koyama et al., 1999). Limbs were fixed with 4% paraformaldehyde overnight, embedded in paraffin, and sectioned. Serial 5 μm-thick sections were pretreated with 1 μg/ml proteinase K (Sigma, St. Louis, MO) in 50 mM Tris-HCl, 5 mM EDTA pH 7.5 for 1 min at room temperature, immediately post-fixed in 4% paraformaldehyde buffer for 10 min, and then washed twice in 1X PBS containing 2 mg/ml glycine for 10 min/wash. Sections were treated for 15 min with a freshly prepared solution

of 0.25% acetic anhydride in triethanolamine buffer. Sections were hybridized with antisense or sense [^{35}S]-labeled riboprobes (approximately 1×10^6 DPM/section) at 50°C for 16 h. cDNA clones used as templates included: a 392 bp mouse *Wnt9a* (547-940; NM_139298); a 550 bp mouse *Gfd5* (1321-1871; NM_008109); a full length mouse *Erg* (AK142379.1); a 211 bp (539-750) or full length mouse β-catenin (MN_007614); a 120 bp mouse collagen IIA (284-404; MN_031163); and a 2,605 bp mouse *lubricin* (41-2646; AB034730). Chick probes were as described (Koyama et al., 1999). After hybridization, slides were washed three times with 2X SSC containing 50% formamide at 50°C for 20 min/wash, treated with 20 μg/ml RNase A for 30 min at 37°C, and washed three times with 0.1X SSC at 50°C for 10 min/wash. Sections were dehydrated by immersion in 70, 90, and 100% ethanol for 5 min/step, coated with Kodak NTB-3 emulsion diluted 1:1 with water, and exposed for 2 days for chick collagen II, 7 days for *lubricin* and 2 to 3 weeks for all remaining genes. Slides were developed with Kodak D-19 at 20°C for 3 min, stained with hematoxylin and eosin, and analyzed and photographed with a Nikon microscope equipped for bright and dark field optics.

Immunohistochemistry

Paraffin sections were de-masked by treatment with 0.2% pepsin in 0.02N HCl for 15 min at 37°C, blocked by incubation with 10% normal goat serum for 1 hr and reacted with a 1:200 dilution of rabbit anti-mouse tenascin-C antiserum (Kalembey et al., 1997) (kindly provided by Dr. T. Yoshida) for 16 hrs at 4°C (Ueta et al., 2001). After washing, bound antibodies were visualized by incubation of biotinylated conjugated goat anti-rabbit IgGs (Vector Labs.) for 30 min at room temperature followed by Cy3-conjugated Streptavidin (Jackson ImmunoResearch Labs.) for 30 min.

RNA isolation and RT-PCR

Total RNA was isolated from tissue or cells by the guanidine isothiocyanate method. First strand cDNA was synthesized from 1 μg of total RNA using 1 μM of random 6 mer primer (Perkin Elmer) using SuperScript II TM reverse transcriptase (Gibco BRL) at 42°C for 45 min. Subsequent elongation was performed with Elongase for 25-35 cycles under the following conditions: 94°C for 30 sec, 58-60°C for 1 min and 68°C for 1 min. Primer sequences for PCR amplification were described previously (Iwamoto et al., 2003) and included the following:

Wnt9a (NM_204981):	F (16) 5′-TTC ATG AGC AGC GCC GGC GCC-3′
	R (800) 5′-GAG CTT TGA GCG ACG TCT CGT AC-3′
Gdf5 (NM_204338):	F(1) 5′-ATG AAA ATC CTG CAT TTT CT-3′
	R (768) 5′-AGA AGA ATG AGA CTT CCA CG-3′
Gli-3 (AF222990):	F (1) 5′-ATG GAG GCC CAG TCC CAC AG-3′
	R (698) 5′-GCT GAC GCC AGC ATG GGG AG-3′
Erg (NM_204280):	F (1056) 5′-GAG GGC ACA AAT GGG GAG TTC AAG-3′
	R 1460) 5′-TGG CAG CCT GGT ATT GGG GTA GAT-3′
Aggrecan (L21913):	F (1040) 5′-GAT GCC ATC TGT TAC AGT GGT GA-3′
	R (1402) 5′ -AGT GCC TGA GAC CGA TGT AGTG -3′
Fibromodulin:	F (395) 5′-TGA AGC AGA GCC TGT CCC TGAA-3′
	R (817) 5′-TTC TCC AGA CCC TCC AGA GCA ATT-3′
CD44 (AF153205):	F (61) 5′-GTT CTG AGG AAA CAA TGG CC-3′
	R (721) 5′-CCA GAA GAA TGA TCT GGC ATA-3′
Col II (MN_204426.1):	F (3614) 5′-CAC CCT CAA ATC CCT CAA CAA TCA G-3′
	R (3873) 5′-TGT CTT TCG TCT TGC TGG TCC ACC-3′
Col IX (M28659):	F (246) 5′-ATT CTG GGT GCT CGT CAA AGA AC-3′
	R (805) 5′-AGC ACT GAG AAG CCA TCA ACA CT-3′
Sox9 (NM_204281):	F (1076) 5′-TAC CTA CGG CAT CAG CAG CTC-3′
	R (1617) 5′-TTG CCT TCA CGT GGC TTT AAG-3′

Interzone cell isolation and culturing

Developing legs were isolated from Day 6.0-6.5 chick embryos and kept in serum-free medium at room temperature. About 0.1 to 0.2 μl of DiI were micro-injected into the metatarsal-

phalangeal and inter-phalangeal interzones under a dissecting microscope, and interzone fragments were dissected out using tungsten needles under Illumatool Bright Light system to visualize labeled tissue. Fragments were collected and treated with 0.15 mg/ml collagenase in DMEM for 30 min at 37°C. The resulting single cell populations were plated at 1×10^5 cells/well in 12-well plates in DMEM containing 10% fetal bovine serum (FBS) and antibiotic mixture and grown for up to 6 days in primary culture. RNA was isolated from 6 day-old cultures and analyzed by semi-quantitative RT-PCR. For *Wnt9a* over-expression studies, insert-less and chick *Wnt9a*-encoding RCAS viruses were grown and concentrated by ultracentrifugation and aliquots were used to infect freshly-isolated interzone cells (Iwamoto et al., 2000). On day 3 to 4 of primary culture, more than 70% of the cells had become infected as revealed by expression of viral antigens. For co-treatment experiments, cells were detached by trypsinization when still subconfluent and re-plated at 1×10^5 cells/well in 48-well plates in complete medium; 1 day later, they were treated with 100 ng/ml of recombinant mouse Gdf-5 (R&D Systems, Inc), 200 ng/ml of recombinant mouse Noggin (R&D Systems, Inc.) or 0.1 μM synthetic human parathyroid-related protein (1-34 fragment) (Peptide Institute, Suita, Japan). Four days after treatment, the cultures were fixed with 10% formalin and stained with alcian blue as described (Iwamoto et al., 2000). Staining levels were digitally measured by Image J software and statistically analyzed by Student's t-test. Above experiments were repeated independently a minimum of 3 times (alcian blue staining) and a minimum of 2 times (RT-PCR).

In additional experiments, interzone fragments and flanking cartilage tissue were dissected out as above and incubated with control virus or *Wnt9a*-encoding RCAS virus in organ culture in low serum medium (1% FBS in DMEM) for up to 3 days. Samples were stained with alcian blue and photographed.

Imaging

Bright and dark-field images of in situ hybridization were taken with a SPOT insight camera (Diagnostic Instruments, Inc.) operated with a SPOT 4.0 software and dark field images were pseudo-colored using Adobe Photoshop software. Live cell images were taken at room temperature using an inverted ECLIPSE TE2000-U Nikon microscope using Image-Pro Plus 6.2 software (Media Cybernetics, Inc.). RT-PCR genes were photographed with a FUJIFILM Luminescent Image Analyzer LAS-1000 plus and digital images were collected using the Image Gauge Version 4.0 plus imaging software (Fuji Photo Film Co. Inc.). No further processing of images was performed apart from assembling montages in Photoshop (version 8, Adobe).

Results

Cell fate tracking

To monitor behavior, roles and fate of limb joint-forming cells, we took advantage of the fact that *Gdf-5* is strongly expressed at the onset of joint formation by interzone cells (Merino et al., 1999; Storm and Kingsley, 1996; Storm and Kingsley, 1999) and expression then persists at reduced levels in most-epiphyseal cells (see below). Thus, we mated *Gdf5-Cre* mice with ROSA-*LacZ* mice and closely monitored the reporter-positive cells at successive prenatal and postnatal stages in resulting double transgenic mice. Whole mount staining clearly showed that reporter activity was predominant in developing metacarpal-phalangeal (*m-ph*), inter-phalangeal (*ph*), wrist (*w*), elbow (*e*) and shoulder (*s*) joints at each stage examined (E13.5 through P28), while the intervening long bone shafts were devoid of reporter-expressing cells (Fig. 1A-F). Histochemical analysis on longitudinal sections (along the proximo-distal limb axis) showed that in E13.5-14.0 specimens the reporter-expressing cells were located at the most epiphyseal ends of phalangeal anlagen (Fig. 2A-B, arrows), but were absent in underlying

cartilaginous shafts that were still structurally young and were being organized into growth plates (Fig. 2A-B, arrowheads). By E17.5 and thereafter (Fig. 2C-F), the positive cells clearly constituted the articular cartilage layers facing the synovial space, were part of adjacent developing joint structures such as synovial lining (*sl*) and capsule tissue (*ct*), but continued to be largely excluded from underlying shafts now containing well defined growth plates (*gp*) and secondary ossification centers (*soc*). Notably, while such preferential distribution of reporter-positive cells invariably characterized the proximal side of each joint, the distal side at times displayed a few positive cells randomly-distributed in the area immediately below the articular layer (Fig. 2E-F).

We noted in early prenatal limbs that the number of reporter-positive cells appeared to vary slightly depending on longitudinal section plane. This raised the intriguing (and previously unsuspected) possibility that joint progenitor cells may not be uniformly distributed along the dorso-ventral axis of incipient joints and interzone. To test this possibility, representative E15.5 *Gdf5-Cre*/ROSA autopods were cross-sectioned and the distribution of reporter-positive cells was systematically monitored in serial sections of metacarpal-phalangeal (*mp*) and inter-phalangeal (*ip*) joints (Fig. 3A). Indeed, the number of reporter-positive cells was much higher in ventral than dorsal half of developing joints (Fig. 3B-E, arrow and double arrow, respectively). The ventral region also displayed tightly-packed masses of reporter-negative cells flanking the joints (Fig. 3C, E, double arrowheads) possibly representing primordia of the outer joint capsule or ligaments. Interestingly, the cavitation process (needed to physically separate the skeletal anlagen and eventually create a synovial space) had initiated on the ventral side, but was unappreciable on the dorsal side (Fig. 3E, arrowhead). Dorsal ventral patterning mechanisms are well known in limb development (Dealy et al., 1993;Parr and McMahon, 1995;Riddle et al., 1995) and may also be important to establish specific functional features of digit joints such as preferential dorsal-to-ventral movement.

Molecular characterization of joint-forming cells

To characterize the phenotypic identity and developmental progression of the joint-forming cells, we carried out gene expression analyses by in situ hybridization. At E15.5 the young joint-forming cells strongly expressed the early joint signaling factors *Wnt9a* and *Gdf5* (Fig. 4A-C, arrow) as well as transcription factor *Erg* (Fig. 4D) (Dhordain et al., 1995; Hartmann and Tabin, 2001; Iwamoto et al., 2000; Storm and Kingsley, 1996). Expression of these genes mirrored the distribution of reporter-positive cells (Fig. 4 G). On the other hand, transcripts encoding *lubricin* were undetectable at this stage (Fig. 4E) reflecting the young age of the joint. By 17.5 and P0, expression of *Wnt9a*, *Gdf5* and *Erg* had become more distinct and largely restricted to the opposing articular layers in each joint (Fig. 4H-K, O-R) and was accompanied by onset of *lubricin* gene expression (Fig. 4L, S), attesting to the fact that the cells were acquiring phenotypic properties characteristics of articular chondrocytes (Jay et al., 2001; Schumacher et al., 1994). By P7, *Wnt9a* and *Gdf5* expression had decreased significantly (Fig. 4V-X), *Erg* expression was maintained by the most-superficial chondrocytes facing the synovial cavity (Fig. 4Y, arrows) and *lubricin* transcripts were now extremely abundant (Fig. 4Z). The acquisition of a functional articular character over developmental time was reiterated by the distribution patterns of tenascin-C (Fig. 4F, M, T and Z'), a pericellular protein characteristic of fetal and adult articular cartilage (Pacifici et al., 1993; Savarese et al., 1996). The above protein and gene expression patterns correlated once again with distribution of reporter-positive cells (Fig. 4N, U, Z"). Notably, while endogenous *Gdf5* expression had significantly decreased postnatally (Fig. 4Q, X), the number of reporter-positive cells continued to be quite prominent (Fig. 4U, Z"), indicating that the cells maintained their joint association and transmitted it to their progeny over time. Similar overall results were obtained in other joints such as the hip joint (Fig. 5). Given the geometry and organization of this large joint, it was more clearly appreciable that the reporter-positive and *lubricin*-expressing cells

were restricted to articulating layers (Fig. 5A-I, arrow) and intra-joint structures such as the teres (Fig. 5D-E, arrowhead).

Isolation of joint-forming cells and functional tests

The above data indicate that the *Gdf5*-expressing reporter-positive cells have the ability to give rise to articular cartilage as well as non-cartilaginous structures such as joint ligaments. To verify that the cells do have such apparent developmental plasticity and to study possible mechanisms, we set out to establish a procedure for isolation of joint progenitor cells and in vitro analysis and testing. We resorted to chick embryos because their limb interzone tissues are more conspicuous, identifiable microscopically in live specimens and microsurgically accessible. To monitor interzone tissue dissection, we first microinjected 0.1-0.2 μl of the vital dye DiI in each metatarsal-phalangeal joint of Day 6.0-6.5 chick embryos (Fig. 6A, arrow). In situ hybridization on companion specimens verified that the interzone tissues were still mesenchymal at this stage and strongly expressed *Gdf5* (Fig. 6B, arrow) but not *collagen II* (Fig. 6C, arrow). DiI-positive joint tissues were then carefully separated from adjacent cartilaginous shafts using custom-made tungsten needles (Fig. 6D, arrow). Effectiveness of this procedure was verified by the fact that the dissected tissues expressed *Gdf5* but not *collagen II* (Fig. 6E-F), thus largely representing joint tissues with minimal if any contamination by shaft cartilage.

Tissues were dissociated into single cell suspensions and the resulting cells were seeded in primary monolayer culture. On day 1, the cells exhibited a fibroblastic appearance as to be expected of mesenchymal cells (Fig. 6G). By day 5, many cells had become round, polygonal and highly refractile (Fig. 6H) that are morphological traits of chondrocytes and expressed typical cartilage genes including *collagens II* and *IX*, *aggrecan*, *fibromodulin* and *Sox 9* (Fig. 6K, left column), suggesting that the cells had a propensity to undergo chondrogenesis and express an articular cartilage-like phenotype.

To determine whether this tendency could be enhanced by chondrogenic factors such as Gdf5 (Merino et al., 1999) but blocked by anti-chondrogenic factors such as Wnt9a (Guo et al., 2004; Hartmann and Tabin, 2001), freshly-isolated cells were treated with recombinant Gdf5 or made to over-express *Wnt9a* using a RCAS retroviral vector. Cells were grown for several days alongside mock-treated companion control cells. Staining with alcian blue revealed that rGdf5-treated cultures (Fig. 6J, c) had accumulated larger amounts of cell-associated proteoglycans than control cultures by day 5 (Fig. 6J, a), a clear sign of enhanced chondrogenesis, whereas there was a clear diminution of staining in *Wnt9a*-over-expressing cultures (Fig. 6J, b). Interestingly, rGdf5 was able to counteract the inhibitory activity of *Wnt9a* (Fig. 6J, d) hinting at possible regulatory interactions between these two cytokines. Indeed, Noggin treatment reduced proteoglycan accumulation in control cultures and reduced it even further in *Wnt9a*-overexpressing cultures (Fig. 6J, e-f). These responses were selective since treatment with PTHrP, a cytokine expressed by periarticular cells (Lanske et al., 1996), had minor effects (Fig. 6J, g-h). Quantification of these observations is shown in Table 1.

RNAs from the day 5 control and *Wnt9a*-overexpressing cultures were processed for semi-quantitative PCR analyses to determine how the morphological and histochemical properties of the cells described above related to their gene expression patterns. Clearly, *Wnt9a*-overexpression caused a marked drop in expression of structural and regulatory cartilage genes including *collagens II* and *IX*, *aggrecan*, *fibromodulin* and *Sox9* (Fig. 6K, right column) compared to control cells (Fig. 6K, left column). Conversely, it caused an appreciable up-regulation of interzone/early joint markers including *CD44*, *Gli3* and *tenascin-C* (Fig. 6L, right column), amounting to 2 to 3 fold after normalization to housekeeping *GAPDH* expression, and a slight increase in *Erg* expression. Interestingly, expression of *Gdf5* was not affected significantly (Fig. 6L, right column). The marked drop in cartilage gene expression and the

increases in interzone gene expression correlated well with the fact that the *Wnt9a*-overexpressing cells all displayed a fibroblastic, flat and highly compacted morphology (Fig. 6I) compared to the chondrocyte-like morphology of their control counterparts (Fig. 6H).

To insure that the interzone cell dissociation procedure did not affect differentiation tendencies and responses, freshly-isolated interzones were maintained in organ culture for up to 3 days in control condition or following infection with *Wnt9a* RCAS virus. For comparison, we isolated cartilage tissue flanking the interzone from the same limbs and reared it in companion cultures. Freshly-isolated interzones were alcian blue-negative, but became positive by day 3; their chondrogenic differentiation was inhibited by *Wnt9a* over-expression (Fig. 6M, top panels) jus as seen in monolayer cultures. Cartilage tissue was already positive after isolation and became extremely positive on day 3; this developmental progression also was inhibited by *Wnt9a* over-expression (Fig. 6M, lower panels), indicating that *Wnt9a* anti-chondrogenic capacity is not restricted to interzone cells but can be broadly effective.

Wnt/β-catenin signaling roles

The above data indicate that when free to act over entire cell populations, Wnt9a action, and Wnt/β-catenin signaling in general, can overwhelm the cells' differentiation program and behavior, raising the question of exactly how this signaling path acts in vivo, how its action is topographically restricted in the developing joints and what its specific targets may be. To examine these issues, we first used the *TOPGAL* and *BATlacZ* reporter mouse lines (DasGupta and Fuchs, 1999; Nakaya et al., 2005) to determine whether, where and for how long Wnt/β-catenin signaling is actually active during joint formation. Whole mount staining clearly revealed that Wnt/β-catenin signaling was active at early stages of joint formation (Fig. 7A-B, arrows) in agreement with previous studies (Guo et al., 2004), and remained active and prominent at later stages as well in small and large joints (Fig. 7C, F, arrows). Interestingly and surprisingly, we observed that signaling activity was particularly strong in most-epiphyseal juxta-articular cells closely abutting the interdigital, wrist or elbow synovial cavities (Fig. 7D-E, G-H).

Next, we created conditional *β-catenin*-deficient mouse embryos by mating *β-catenin*-floxed mice (*β-cat*$^{fl/fl}$) with *Col2a1-Cre* or *Gdf5-Cre* mice (Figs. 8-9, respectively). Limb joints including elbows, knees and digits did form in both mutants. While most joints appeared largely normal anatomically, some fusion was observed in the wrist area of *β-cat*$^{fl/fl}$;*Col2a1-Cre* limbs (Fig. 8Z") compared to wild type (Fig. 8M). In addition, close histological inspection revealed that the organization of cells in most joints was appreciably different in mutant versus wild type. For example, joint cells in wild type E15.5 and E17.5 elbow or wrist displayed a typical stratified organization and distinct cell morphologies, with those immediately facing the synovial cavity displaying a more flattened cytoarchitecture and those present underneath displaying a more round and chondrocytic morphology (Fig. 8A-B, arrows). In *β-cat*$^{fl/fl}$;*Col2a1-Cre* mutant joints (4/7), the number of flattened cells was lower and most of the joint-facing cells exhibited a rounder shape (Fig. 8O-P, arrows). Phalangeal joints were less affected (not shown). These subtle morphological differences were fully consistent with the finding that the mutant joints exhibited an appreciable reduction in *Erg* and *Gdf5* gene expression and a marked reduction in *collagen IIA* and *lubricin* gene expression (Fig. 8Q-X and Z'-Z") compared to wild type littermate specimens (Fig. 8C-J and M-N). Endogenous β-catenin transcripts were much reduced in mutant tissues (Fig. 8Y-Z) compared to controls (Fig. 8K-L) as to be expected. A similar reduction in flattened cell layer and lubricin expression was seen in some *β-cat*$^{fl/fl}$;*Gdf5-Cre* mutant joints (Fig. 9E-H, arrows) (2/3) compared to controls (Fig. 9A-D, arrows).

Discussion

It has long been appreciated that articular cartilage and other joint tissues are structurally and functionally different from shaft and growth plate cartilage. The former are composed of phenotypically stable cells that provide continuous function through life, while shaft and growth plate cartilage is made of highly dynamic transient chondrocytes that undergo maturation, hypertrophy and apoptosis and are eventually replaced by endochondral bone and marrow. The data in the present study reaffirm and greatly extend our previous findings (Rountree et al., 2004) that such functional differences involve distinct developmental origins. Articular chondrocytes and other joint cells appear to derive from *Gdf5*-expressing joint progenitor cells and/or their descendants, whereas shaft and growth plate cartilage derives for the most part from *Gdf5*-negative cells likely representing the bulk of the original condensed limb mesenchyme. The *Gdf5*-expressing and reporter-positive cells thus act as a specialized and distinct cohort of limb skeletal progenitor cells devoted to joint formation (Barna et al., 2005) and display the dual ability of remaining topographically confined to joint formation sites while at the same time undergoing differentiation in joint tissues. At early stages the cells strongly express genes such as *Wnt9a* and *Erg* in addition to *Gdf5*. With time and development, the cells down-regulate expression of these early regulatory genes, while expression of structural genes such as *lubricin, tenascin-C* and *collagen II* becomes preponderant. Clearly, the patterning and topographical means by which the cells arise and reside at specific joint-forming locations in the limb co-exist with mechanisms by which the cells progress from a mesenchymal and undifferentiated character to a functional and differentiated character.

As our data indicate, *Gdf5* expression is first evident in the mesenchymal interzone of early joints and continues for a few additional days in emerging joint structures including most-epiphyseal articular layers and neighboring cells (Fig. 4). Since *Gdf5*-driven *Cre* is followed by irreversible activation of reporter activity, our data do not allow us to establish exactly what developmental relationship exists amongst the reporter-positive cell populations. One possibility is that the initial mesenchymal *Gdf5*-expressing interzone cells serve as the founders of all joint-forming cells, and every differentiated tissue including articular cartilage and synovial lining would directly descend from them. A second possibility is that there are distinct joint-associated *Gdf5*-expressing subpopulations emerging at successive stages and/or distinct locations that will give rise to different joint tissues. At this regard, it is important to point out a very recent paper examining the embryological origin of articular chondrocytes in mouse embryos (Hyde et al., 2007). The authors exploited the fact that the matrix component matrillin-1 is not expressed by developing articular chondrocytes, but is expressed by underlying epiphyseal and growth plate chondrocytes. Using *matrillin-1-Cre* mice mated with ROSA-*LacZ* mice, they found that *matrillin-1*- and reporter-negative chondrocytes were already appreciable in early knee joints in E13.5 mouse embryos and flanked the interzone, and cells with similar phenotype could be seen at subsequent stages (Hyde et al., 2007). The authors concluded that articular chondrocytes arise from a subpopulation of early chondrocytes part of the original anlagen as proposed previously (Bland and Ashhurst, 1996), but do not derive from the dispersal of flattened interzone cells as suggested by others (Ito and Kida, 2000). This conclusion is plausible and certainly our data also point to the fact that articular chondrocytes and joint cells in general represent a separate and distinct cohort of limb skeletal-forming cells. However, since the articular cells were defined by lack of a phenotypic trait (matrillin-1) and could not be monitored over time, their exact origin and their relationship to interzone cells is not as certain as the authors proposed, and as we point above, this issue remains to be solved.

One reason why the exact roles of interzone cells in joint formation remain unclear and controversial is that their biological properties and possible functions have been inferred from in vivo studies such as those above, rather than by direct isolation and study of the cells

themselves. Thus, the observations we report here using primary cultures of *Gdf5*-positive progenitor cell populations isolated from chick interzone tissue are rather novel. Our data indicate that the cells display a propensity to differentiate into chondrocytes under the monolayer and explant conditions used, and this tendency is reinforced by rGdf5 treatment. In contrast, forced expression of *Wnt9a* prevents their differentiation into chondrocytes (Guo et al., 2004; Spater et al., 2006a), maintains their initial progenitor mesenchymal character, and stimulates expression of interzone/joint traits such as *CD44, Gli-3, collagen II, tenascin-C* and to a lesser extent *Erg*. Based on these responses, interzone cells appear to be phenotypically malleable and can be steered into distinct developmental programs by different signaling pathways. This flexibility could represent a major developmental asset if, as pointed out above, the cells were to serve as the founders of distinct joint cell lineages and give rise to both chondrogenic structures such as articular cartilage and non-chondrogenic tissues such as intra-joint ligaments and synovial lining (see our model in Fig. 10). We showed recently that rGdf5 is a potent and rapid inducer of *Erg* gene expression (Iwamoto et al., 2007), and our data here indicate that *Wnt9a* is a strong inducer of other joint-associated genes above. These observations lend further support to the notion that joint progenitor cell function and joint formation are orchestrated by factors with strong and quite distinct biological activity and potency (Settle et al., 2003; Spater et al., 2006b). What remains to be worked out then is how these factors and the several others expressed by incipient joints (Pacifici et al., 2005) would operate within the developing joint and eventually lead to the formation of distinct joint tissues with appropriate location, structure, organization and morphology.

In this regard, several previous studies have aimed to define the roles of Wnt/β-catenin signaling in joint formation. Initial studies suggested that Wnt/β-catenin signaling is required and sufficient for induction of joint formation based on partial joint fusion seen in *β-cat*$^{fl/fl}$;*Col2a1-Cre* and severe joint fusion/ablation seen in *β-cat*$^{fl/fl}$;*Dermo1-Cre* embryos (Guo et al., 2004). However, subsequent studies on *β-cat*$^{fl/fl}$;*Prx1-Cre* and *Wnt9a/Wnt4* double-null embryos led to the conclusion that Wnt signaling may not be needed for initiation of joint formation, but would be important for long-term joint integrity (Spater et al., 2006a; Spater et al., 2006b). Given that joints form in our *β-cat*$^{fl/fl}$;*Col2-Cre* and *β-cat*$^{fl/fl}$;*Gdf5-Cre* mice and some joint fusion/ablation is observed in the wrist area only, our data appear to lend more support to the latter studies, though we cannot rule out that Wnt/β-catenin signaling could have acted at a very early stage prior to *Cre* activation in our mice. In addition, differences in phenotypic severity seen amongst different studies may reflect use of broader-acting Cre lines such as *Dermo1-Cre* and *Prx1-Cre* lines when compared to a more selective line such as *Col2a1-Cre*. In any case, we do find that β-catenin signaling is not only present at early joint formation stages (Guo et al., 2004), but persists at later stages and is particularly strong in the cell layers immediately facing the synovial cavity. In good agreement, we find also that the β-catenin-deficient joints have some defects in those layers and exhibit reduced levels of *lubricin* and *collagen IIA* expression. The findings suggest that a persistent level of β-catenin signaling may be beneficial for completion of joint formation and could be of particular importance for generation and/or maintenance of the superficial cell layers (see model in Fig. 10). We should note here that even in the adult organism, articular cartilage is not a homogenous tissue and is characterized by structurally and functionally distinct layers or zones. The adult surface layer is made of flat discoid cells and is the site of continuous production of lubricin and other joint lubricating molecules such as hyaluronan (Schumacher et al., 1994), whereas the intermediate zone contains typical round chondrocytes producing aggrecan, collagen IIB and other major matrix products (Lorenzo et al., 1998). Despite the importance of such structural and functional stratification for joint functioning through life, it has not been clear how articular cartilage actually acquires such layered organization to begin with. Our data indicate that β-catenin signaling could be a factor in the formation and possibly long-term maintenance of a superficial flat cell layer (Fig. 10). Significant interest has been generated by previous observations indicating that the superficial zone of articular cartilage and synovial

tissue in adults contain stem/progenitor cells that could potentially serve as a reservoir for cartilage maintenance, repair or regeneration (Dowthwaite et al., 2004; Nishimura et al., 1999). Given that Wnt/β-catenin signaling maintains interzone cells in a mesenchymal status as we show here, it is possible that such pathway could also be involved in maintaining the long-term developmental potentials of those cells and could do so together with mechanisms such as Notch signaling (Hayes et al., 2003).

Recent data shows that human variation in *GDF5* sequence and expression is significantly associated with risk of adult onset osteoarthritis of the hip and knee in several different populations (Miyamoto et al., 2007; Southam et al., 2007). Better understanding of the origin, fate and function of *Gdf5*-expressing cells thus provides and will continue to provide new insights not only into early formation of joint tissues, but also into an important risk factor for one of the most common skeletal diseases in humans.

Acknowledgements

We express our gratitude to: Ms. A. Hargett and J. Williams for technical assistance; Dr. T. Yoshida for providing the mouse tenascin-C antibodies; Dr. Y. Yamada for the *Col2a1-Cre* mice; Dr. T. E. Yamaguchi for the *BATLacz* mice; and to Dr. C. Tabin for the chick *Wnt9a* RCAS plasmid. This work was supported by National Institutes of Health grants AG025868, AR046000, AR050507 and AR042236. D.M.K. is an investigator of the Howard Hughes Medical Institute.

References

Barna M, Pandolfi PP, Niswander L. Gli3 and Plzf cooperate in proximal limb patterning at early stages of limb development. Nature 2005;436:277–281. [PubMed: 16015334]

Bird HA. Controversies in the treatment of osteoarthritis. Clin. Rheum 2003;22:165–167.

Bland YA, Ashhurst d. E. Development and ageing of the articular cartilage of the rabbit knee joint: distribution of fibrillar collagens. Anat. Embryol 1996;194:607–619. [PubMed: 8957536]

Brandt KD. Non-surgical treatment of osteoarthritis: a half century of “advances”. Annu. Rheum. Dis 2004;63:117–122.

Brunet LJ, McMahon JA, McMahon AP, Harland RM. Noggin, cartilage morphogenesis, and joint formation in the mammalian skeleton. Science 1998;280:1455–1457. [PubMed: 9603738]

Buckwalter JA, Martin JA, Brown TD. Perspectives on chondrocyte mechanobiology and osteoarthritis. Biorheology 2006;43:603–609. [PubMed: 16912432]

Dangleish, AE. Development of the limbs of the mouse. Stanford Univ. Press; Stanford, CA: 1964.

DasGupta R, Fuchs E. Multiple roles of activated LEF/TCF transcription complexes during hair follicle development and differentiation. Development 1999;126:4557–4568. [PubMed: 10498690]

Dealy CN, Roth A, Ferrari D, Brown AMC, Kosher RA. Wnt-5a and Wnt-7a are expressed in the developing chick limb bud in a manner that suggests roles in pattern formation along the proximodistal and dorsoventral axes. mech. Dev 1993;43:175–186. [PubMed: 8297789]

Dhordain P, Dewitte F, Desbiens X, Stehelin D, Duterque-Coquillaud M. Mesodermal expression of the chicken *erg* gene associated with precartilaginous condensation and cartilage differentiation. Mech. Dev 1995;50:17–28. [PubMed: 7605748]

Dowthwaite GP, Bishop JC, Redman SN, Khan IM, Rooney P, Evans DJR, Haughton L, Bayram Z, Boyer S, Thomson B, Wolfe MS, Archer CW. The surface of articular cartilage contains a progeniotr cell population. J. Cell Sci 2004;117:889–897. [PubMed: 14762107]

Guo X, Day TF, Jiang X, Garrett-Beal L, Topol L, Yang Y. Wnt/β-catenin signaling is sufficient and necessary for synovial joint formation. Genes Dev 2004;18:2404–2417. [PubMed: 15371327]

Hamrick MW. Primate origins: evolutionary change in digital ray patterning and segmentation. J. Hum. Evol 2001;40:339–351. [PubMed: 11312586]

Hartmann C, Tabin CJ. Wnt-14 plays a pivotal role in inducing synovial joint formation in the developing appendicular skeleton. Cell 2001;104:341–351. [PubMed: 11239392]

Hayes AJ, Dowthwaite GP, Webster SV, Archer CW. The distribution of Notch receptors and their ligands during articular cartilage development. J. Anat 2003;202:495–502. [PubMed: 12846471]

Hinchliffe, JR.; Johnson, DR. The Development of the Vertebrate Limb. Oxford University Press; New York: 1980. p. 72-83.

Holder N. An experimental investigation into the early development of the chick elbow joint. J. Embryol. Exp. Morphol 1977;39:115–127. [PubMed: 886251]

Hyde G, Dover S, Aszodi A, Wallis GA, Boot-Handford RP. Lineage tracing using matrillin-1 gene expression reveals that articular chondrocytes exist as the joint interzone forms. Dev. Biol 304:825–833. [PubMed: 17313942]

Ito MM, Kida MY. Morphological and biochemical re-evaluation of the process of cavitation in the rat knee joint: cellular and cell strata alterations in the interzone. J. Anat 2000;197:659–679. [PubMed: 11197539]

Iwamoto M, Higuchi Y, Koyama E, Enomoto-Iwamoto M, Yeh H, Abrams WR, Rosenbloom J, Pacifici M. Transcription factor ERG variants and functional diversification of chondrocytes during long bone development. J. Cell Biol 2000;150:27–39. [PubMed: 10893254]

Iwamoto M, Kitagaki J, Tamamura Y, Gentili C, Koyama E, Enomoto H, Komori T, Pacifici M, Enomoto-Iwamoto M. Runx2 expression and action in chondrocytes are regulated by retinoid signaling and parathyroid hormone-related peptide (PTHrP). Osteoarthr. Cart 2003;11:6–15.

Iwamoto M, Tamamura Y, Koyama E, Komori T, Takeshita N, Williams JA, Nakamura T, Enomoto-Iwamoto M, Pacifici M. Transcription factor ERG and joint and articular cartilage formation during mouse limb and spine skeletogenesis. Dev. Biol 2007;305:40–51. [PubMed: 17336282]

Jay GD, Tantravahi U, Britt DE, Barrach HJ, Cha CJ. Homology of lubricin and superficial zone protein (SZP): products of megakaryocyte stimulating factor (MSF) gene expression by human synovial fibroblasts and articular chondrocytes localized to chromosome 1q25. J. Orthop. Res 2001;19:677–687. [PubMed: 11518279]

Koyama E, Golden EB, Kirsch T, Adams SL, Chandraratna RAS, Michaille J-J, Pacifici M. Retinoid signaling is required for chondrocytematuration and endochondral bone formation during limb skeletogenesis. Dev. Biol 1999;208:375–391. [PubMed: 10191052]

Lanske B, Karaplis AC, Lee K, Lutz A, Vortkamp A, Pirro A, Karperien M, Defize LHK, Ho C, Mulligan R, Abou-Samra AB, Juppner H, Segre GV, Kronenberg HM. PTH/PTHrp receptor in early development and Indian hedgehog-regulated bone growth. Science 1996;273:663–666. [PubMed: 8662561]

Lorenzo P, Bayliss MT, Heinegard D. A novel cartilage protein present in the mid-zone of human articular cartilage increases with age. J. Biol. Chem 1998;273:23463–23468. [PubMed: 9722583]

Merino R, Macias D, Ganan Y, Economides AN, Wang X, Wu Q, Stahl N, Sampath TK, Varona P, Hurle JM. Expression and function of Gdf-5 during digit skeletogenesis in the embryonic chick leg bud. Dev. Biol 1999;206:33–45. [PubMed: 9918693]

Mitrovic D. Development of the diathrodial joints in the rat embryo. Am. J. Anat 1978;151:475–485. [PubMed: 645613]

Miyamoto Y, Mabuchi A, Shi D, Kubo T, Takatori Y, Saito S, Fujioka M, Sudo A, Uchida A, Yamamoto S, Ozaki K, Takigawa M, Tanaka T, Nakamura Y, Jiang O, Ikegawa S. A functional polymorphism in the 5′ UTR of GDF5 is associated with susceptibility to osteoarthritis. Nat. Genet 2007;39:529–533. [PubMed: 17384641]

Nakaya MA, Biris K, tsukiyama T, Jaime S, Rawls JA, Yamaguchi TP. Wnt3a links left-right determination with segmentation and anteroposterior axis elongation. Development 2005;132:5425–5436. [PubMed: 16291790]

Nishimura K, Solchaga LA, Caplan AI, Yoo JU, Goldberg VM, Johnstone B. Chondroprogenitor cells of synovial tissue. Arthr. Rheum 1999;42:2631–2637. [PubMed: 10616011]

Pacifici M, Iwamoto M, Golden EB, Leatherman JL, Lee Y-S, Chuong C-M. Tenascin is associated with articular cartilage development. Dev. Dynam 1993;198:123–134.

Pacifici M, Koyama E, Iwamoto M. Mechanisms of synovial joint and articular cartilage formation: recent advances, but many lingering mysteries. Birth Defects Research 2005;75(Pt C):237–248. [PubMed: 16187328]

Parr BA, McMahon AP. Dorsalizing signal wnt-7a required for normal polarity of D-V and A-P axes of the mouse limb. Nature 1995;374:350–353. [PubMed: 7885472]

Riddle RD, Ensini M, Nelson CE, Tsuchida T, Jessell TM, Tabin CJ. Induction of the LIM homeobox gene Lmx1 by WNT7a establishes the dorsoventral pattern in the vertebrate limb. Cell 1995;83:631–640. [PubMed: 7585966]

Rountree RB, Schoor M, Chen H, Marks ME, Harley V, Mishina Y, Kingsley DM. BMP receptor signaling is required for postnatal maintenance of articular cartilage. PLoS Biology 2004;2:1815–1827.

Savarese JJ, Erickson H, Scully SP. Articular chondrocyte tenascin-C production and assembly into de novo extracellular matrix. J. Orthop. Res 1996;14:273–281. [PubMed: 8648506]

Schumacher BL, Block JA, Schmid TM, Aydelotte MB, Kuettner KE. A novel proteoglycan synthesized and secreted by chondrocytes of the superficial zone of articular cartilage. Arch. Biochem. Biophys 1994;311:144–152. [PubMed: 8185311]

Serra R, Johnson M, Filvaroff EH, LaBorde J, Sheehan DM, Derynck R, Moses HL. Expression of a truncated, kinase-defective TGF-β type II receptor in mouse skeletal tissue promotes terminal chondrocyte differentiation and osteoarthritis. J. Cell Biol 1997;139:541–552. [PubMed: 9334355]

Settle SH, Roundtree RB, Sinha A, Thacker A, Higgins K, Kingsley DM. Multiple joint and skeletal patterning defects caused by single and double mutations in the mouse *Gdf5* and *Gdf6* genes. Dev. Biol 2003;254:116–130. [PubMed: 12606286]

Soriano P. Generalized lacZ expression with the ROSA26 Cre reporter strain. Nat. Genet 1999;21:70–71. [PubMed: 9916792]

Southam L, Rodriguez-Lopez J, Wilkins JM, Pombo-Suarez M, Snelling S, Gomez-Reino JJ, Chapman K, Gonzalez AM, Loughlin J. A SNP in the 5′ UTR of *GDF5* is associated with osteoarthritis susceptibility in Europeans and with in vivo differences in allelic expression in articular cartilage. Hum. Mol. Genet. 2007Epub ahead of print

Spagnoli A, O'Rear L, Chandler RL, Granero-Molto F, Mortlock DP, Gorska AE, Weis JA, Longobardi L, Chytil A, Shimer K, Moses HL. TGF-β signaling is essential for joint morphogenesis. J. Cell Biol 2007;177:1105–1117. [PubMed: 17576802]

Spater D, Hill PT, Gruber M, Hartmann C. Role of canonical Wnt-signaling in joint formation. Eur. Cells Materials 2006a;12:71–80.

Spater D, Hill TP, O'Sullivan RJ, Gruber M, Conner DA, Hartmann C. Wnt9a signaling is required for joint integrity and regulation of Ihh during chondrogenesis. Development 2006b;133:3039–3049. [PubMed: 16818445]

Storm EE, Huynh TV, Copeland NG, Jenkins NA, Kingsley DM, Lee S. Limb alterations in brachypodism mice due to mutations in a new member of the TGFβ-superfamily. Nature 1994;368:639–643. [PubMed: 8145850]

Storm EE, Kingsley DM. Joint patterning defects caused by single and double mutations in members of the bone morphogenetic protein (BMP) family. Development 1996;122:3969–3979. [PubMed: 9012517]

Storm EE, Kingsley DM. GDF5 coordinates bone and joint formation during digit development. Dev. Biol 1999;209:11–27. [PubMed: 10208739]

Thomas JT, Kilpatrick MW, Lin K, Erlacher L, Lembessis P, Costa T, Tsipouras P, Luyten FP. Disruption of human limb morphogenesis by a dominant negative mutation in CDMP1. Nat. Genet 1997;17:58–64. [PubMed: 9288098]

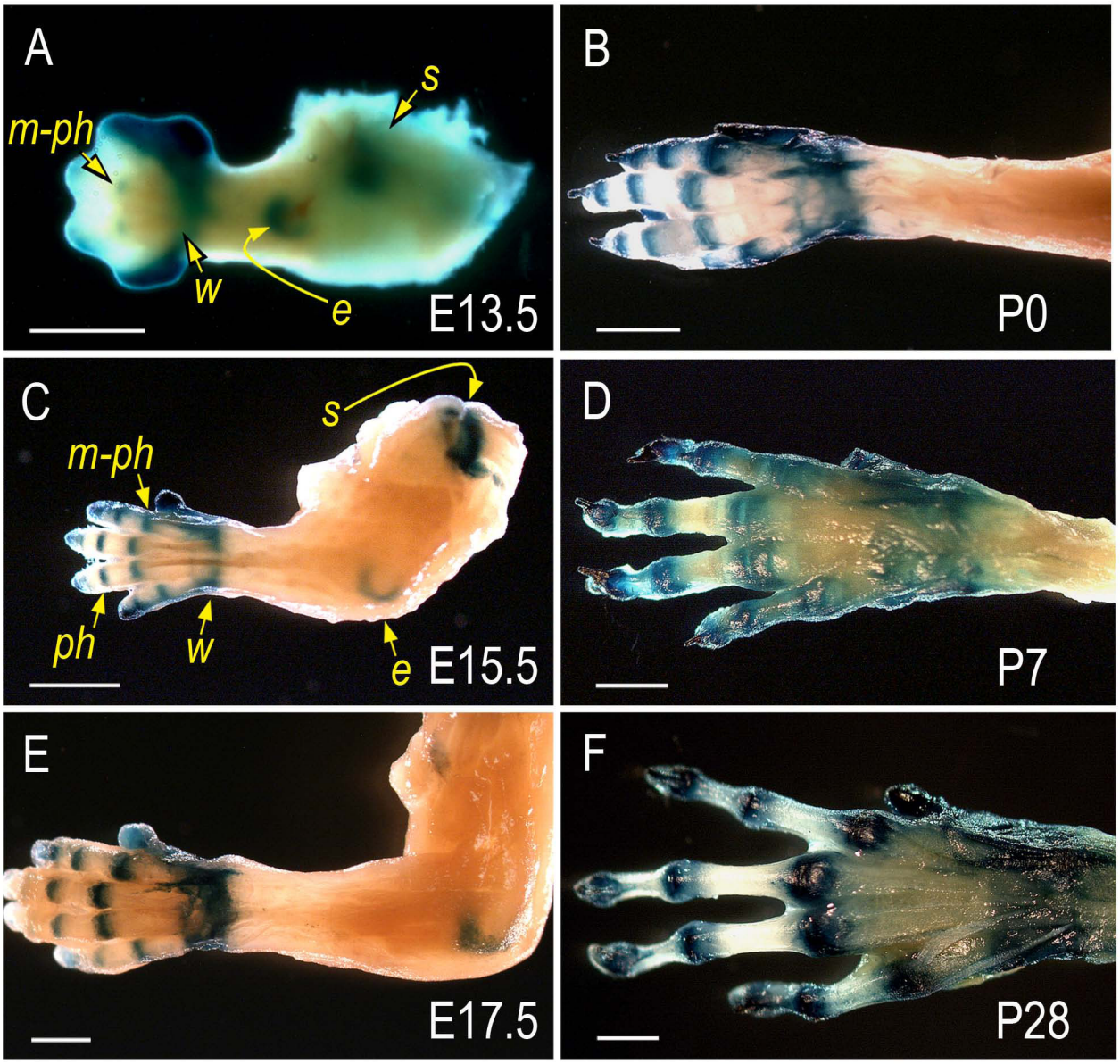

Fig. 1.

Reporter-expressing cells are predominant in developing joints pre-natally and post-natally. Limbs isolated from the progeny of ROSA R26R mice mated with *Gdf5-Cre* mice were processed for whole mount detection of *β*-galactosidase activity. (A) At E13.5, reporter activity is distinctly visible in incipient joints at the prospective metacarpal-phalangeal (*m-ph*), wrist (*w*), elbow (*e*) and shoulder (*s*) sites. (C and E) By E15.5 and E17.5, reporter activity is clearly restricted at sites of joint formation that now include also the inter-phalangeal (*ph*) site. (B, D and F). Preferential location of reporter activity persists at every postnatal time point examined including P0, P7 and P28. Bars, 1 mm.

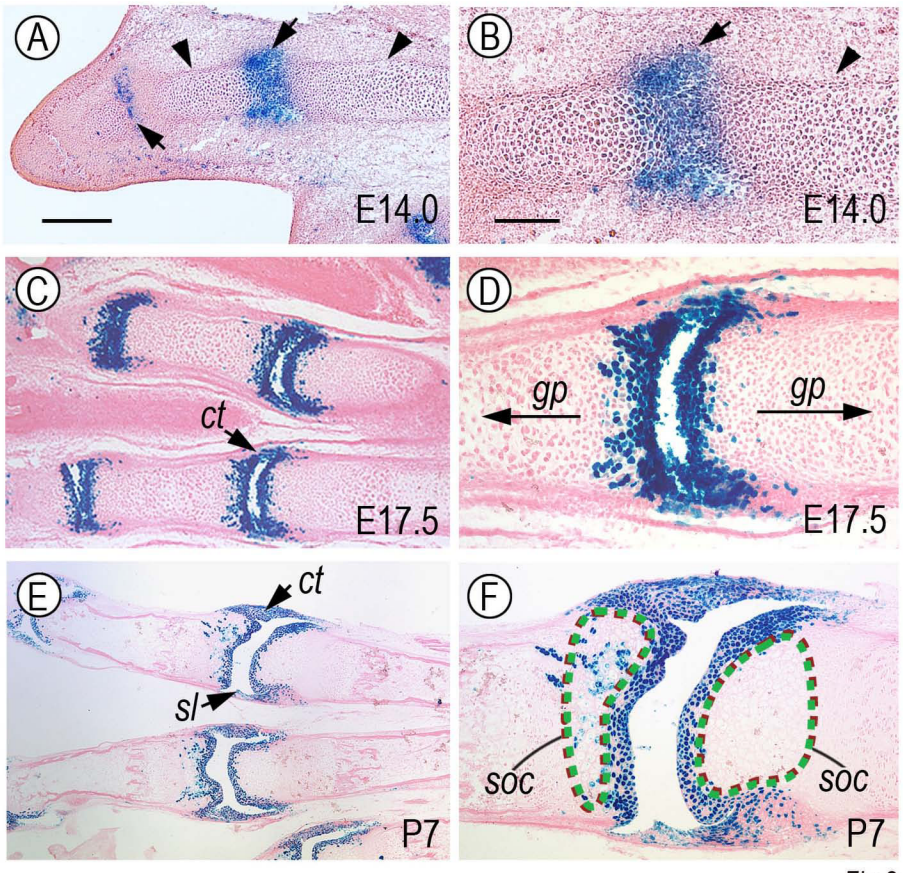

Fig. 2.

Reporter-expressing cells are predominant in articulating layers and accessory joint tissues. Longitudinal sections from representative forelimb autopod specimens similar to those in Fig. 1 were processed for histochemical detection of *β*-galactosidase activity. In each joint, proximal side is on the right and distal side is on the left. (A) At E14.0, reporter-positive cells are predominant in nascent metacarpal-phalangeal and inter-phalangeal joint sites (*arrows*), but are undetectable in the flanking cartilaginous shafts (*arrowheads*). (C and E) By E17.5 and P7, the reporter-positive cells clearly constitute the 3 to 4 articular cell layers facing the incipient joint space and cavity and are present in accessory joint tissues such as synovial lining (*sl*) and capsule tissue (*ct*). (B, D and F) These are higher magnification views of images shown in panels A, C and E, respectively. Note that the reporter-positive cells are limited to nascent joint tissue at E14.0 (B) and to joint-facing articular layers and associated joint tissues at E17.5 and P7 (D and F). Note also that while the positive cells are excluded from growth plates and incipient secondary ossification center (*soc*) on the distal side, a few positive cells are also present in the sub-articular epiphyseal/*soc* area on the proximal side. Apparent size of synovial space may have become enlarged during tissue processing, particularly in specimen shown in E and F. Bar for A, C and E, 200 μm; bar for B, D and F, 75 μm.

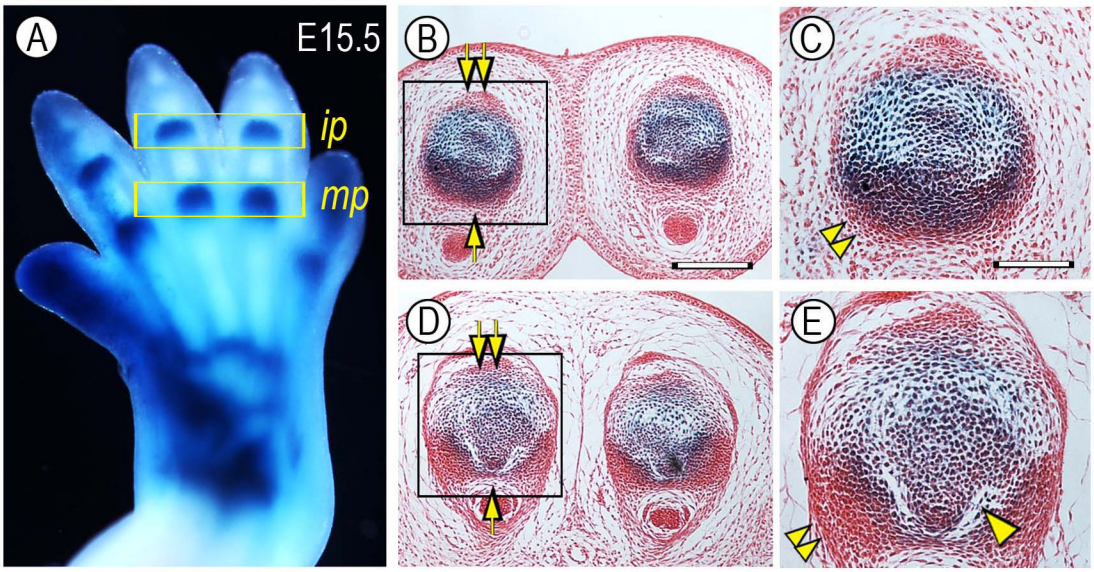

Fig. 3.

Reporter-expressing cells are more numerous ventrally than dorsally. (A) Whole mount staining of a E15.5 *Gdf5-Cre*/ROSA forelimb in which developing metacarpal-phalangeal (*mp*) and inter-phalangeal (*ip*) joints are strongly positive. Histological cross sections of *ip* joints (B-C) and *mp* joints (D-E) show that there are more numerous reporter-positive cells in the ventral half (*arrow*) than dorsal half (*double arrow*). Note also: the presence of tightly-packed ventro-lateral cell masses (double arrowhead) possibly representing prospective capsule precursors; and initiation of cavitation process in the ventral side (*arrowhead*). Bar for B and D, 250 μm; bar for C and E, 110 μm.

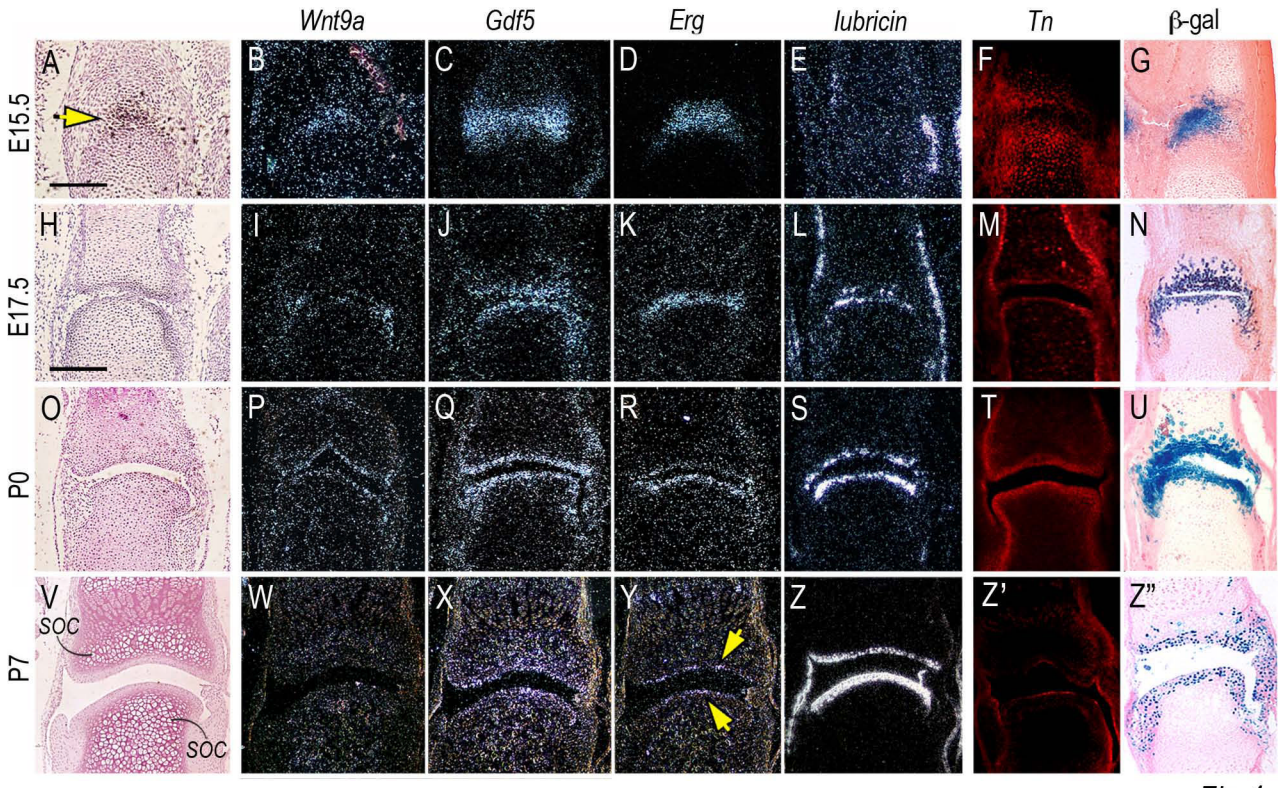

Fig. 4.

Reporter-expressing cells acquire articular chondrocyte characteristics over developmental time. Longitudinal serial sections from fetal and postnatal autopods were processed for histology and in situ hybridization. Sections from companion specimens were processed for immunohistochemical detection of tenascin-C (*Tn*) or histochemical detection of *β*-galactosidase-positive (*β*-gal) cells. (A-G) At E15.5, interzone cells (yellow arrow in A) express *Wnt9a*, *Gdf5* and *Erg*, are part of tenascin-C-containing epiphyseal tissue (F), display strong and distinct *β*-galactosidase activity (G), but lack detectable *lubricin* expression (E). (H-N and O-U) At E17.5 and P0, expression of *Wnt9a*, *Gdf5* and *Erg* is clearly restricted to articular cells that display also *lubricin* transcripts (L and S), distinct tenascin-C content (M and T) and strong *β*-galactosidase activity (N and U). (V-Z") By P7, *Wnt9a* and *Gdf5* expression is markedly down-regulated (W-X), *Erg* expression is maintained in cells abutting the synovial space (Y, *arrows*), while *lubricin* expression remains strong throughout the articulating layer (Z) that also contains tenascin-C (Z') and *β*-galactosidase-expressing cells (Z"). Note in (V) the prominent secondary ossification centers (*soc*) visible immediately below the articular layers. Bar for A-G, 150 μm; bar for H-Z", 100 μm.

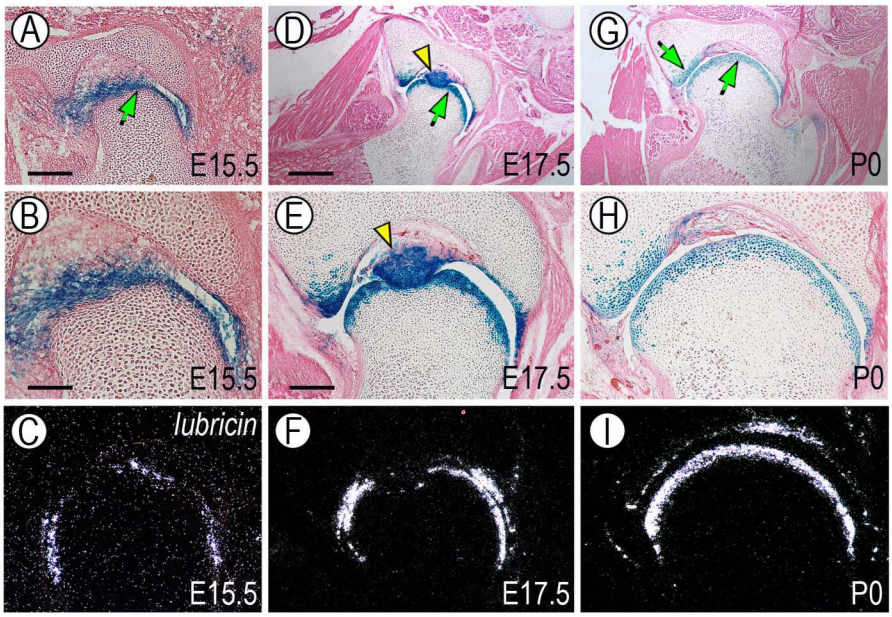

Fig. 5.

Cell fate-map analysis during hip joint development. Cross sections of hip joint region from E15.5, E17.5 and P0 animals were processed for histochemical detection of *β*-galactosidase-positive cells. Similar sections from companion animals were processed for in situ hybridization analysis of lubricin gene expression. (A, D and G) Positive cells are restricted to the articular layers facing the synovial cavity (*arrows*) and constitute also the teres which is the main femoral head's ligament (*arrowhead*). (B, E and H) Higher magnification view of the above sections clearly shows that the reporter-positive cells are confined to 3 to 4 layers facing the joint cavity. (C, F and I) Lubricin gene expression is confined to joint associated cells. Distribution of lubricin-expressing cells is clearly reminiscent and virtually over-lapping that of reporter-positive cells. Bar for A, 175 μm; bar for B-C, 75 μm; bar for D and G, 350 μm; bar for E-F and H-I, 150 μm.

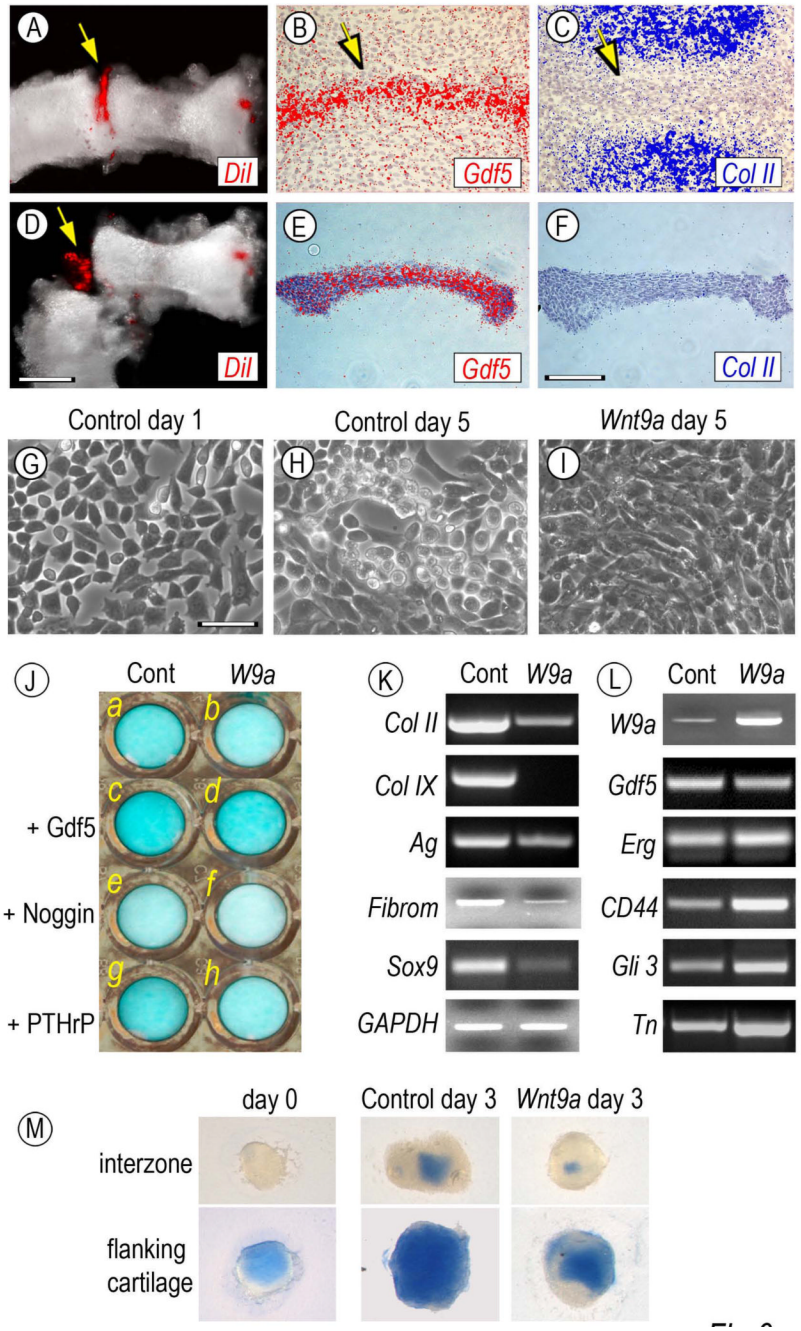

Fig. 6.

Isolation, culturing and testing of interzone-associated cells. Metatarsal and first inter-phalangeal interzones present in Day 6.5 chick embryo leg buds were microinjected with DiI (A, *arrow*) and were dissected out by means of custom-made tungsten needles (D, *arrow*). In situ hybridization on companion specimens shows that prior to dissection, the interzone tissue strongly expressed *Gdf5* (B, *arrow*) but not *collagen II* (C, *arrow*); note that hybridization signal is pseudo-colored. These patterns were maintained in isolated tissue (E-F). On day 1 of culture, interzone tissue-derive cells displayed a fibroblastic-mesenchymal morphology (G), acquired a chondrocytic phenotype by day 5 (H), but retained a mesenchymal appearance after infection with *Wnt9a*-encoding RCAS virus (I). In J, companion control and *Wnt9a*-

overexpressing cultures in multi-well plates were treated with 100 ng/ml rGdf5 (*c-d*), 200 ng/ml Noggin (*e-f*) or 0.1 μM PTHrP (*g-h*) or were left untreated (*a-b*). Fresh cytokines were given on day 1 and all cultures were stained with alcian blue on day 5. Note that exogenous rGdf5 increases proteoglycan content (*c*) and counteracts the *Wnt9a*-induced loss of proteoglycan staining (*d*), while Noggin treatment leads to a marked decrease in staining in both cultures (*e-f*). (K-L) RT-PCR analysis of genes expressed in day 5 control or *Wnt9a*-over-expressing cultures. Note that *Wnt9a*-overexpression leads to a marked down-regulation of chondrocyte-characteristic genes including *collagen II* (*Col II*) *collagen IX* (*Col IX*), *aggrecan* (*Ag*), *fibromodulin* (*Fibrom*) and *Sox9*, but causes an up-regulation of early joint/interzone-characteristic genes including *CD44*, *Gli3* and *tenascin-C* (*Tn*) and a modest increase in *Erg* expression. (M) Explant cultures of interzones and flanking cartilage tissue stained with alcian blue after isolation (day 0) or after 3 days in culture with infection with insert-less or *Wnt9a* RCAS virus. Bar for A and D, 300 μm; bar for B-C and E-F, 150 μm; bar for G-I, 30 μm.

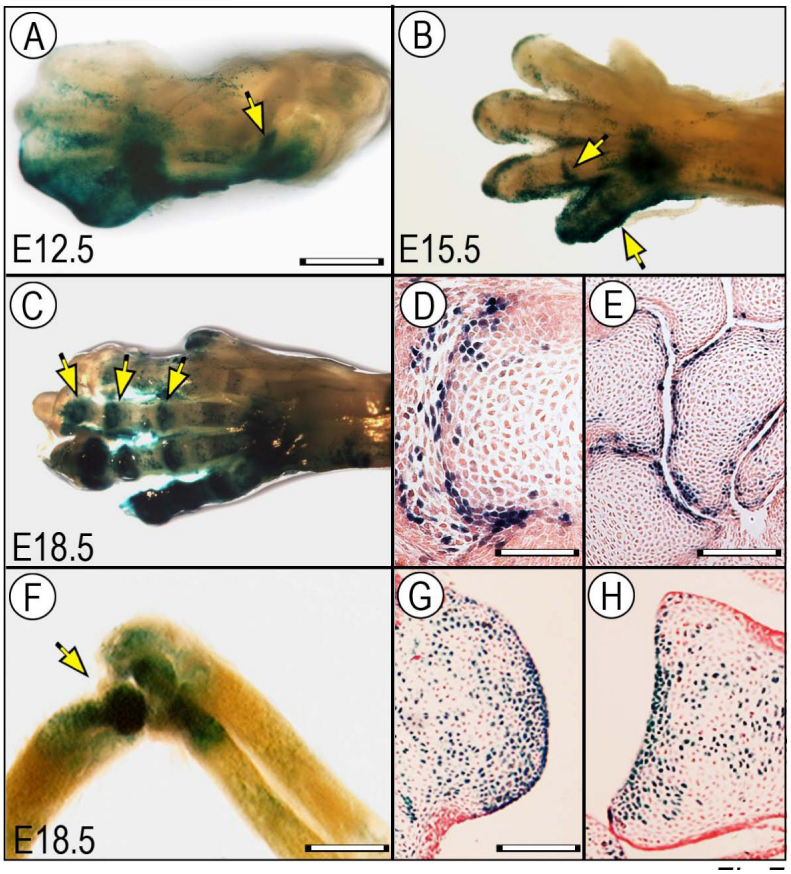

Fig. 7.

Wnt/*β*-catenin signaling is active at multiple stages of joint formation. Limbs from *BATlacZ* (A-E) and *TOPGAL* (F-H) Wnt-*β*-catenin reporter mouse embryos were processed for whole mount *β*-galactosidase (*β-gal*) staining (A-C, F) or section staining (D-E, G-H). (A) At E12.5, *β-gal* activity is already detectable in developing large joints such as the elbow (arrow). (B-E) By E15.5 and E18.5, activity is clearly visible in digit joint also (B-C, arrows) and is particularly strong in joint cells abutting the nascent interdigital and wrist joint cavities (D-E). (F-H) At E18.5, activity remains strong in large joints such as elbow (F) and characterizes articular cells all along the joint surface and neighboring cells (G-H). Bar for A-C, 1 mm; bar for D, 150 μm; bar for E, 300 μm, bar for F, 0.8 mm; bar for G-H, 250 μm.

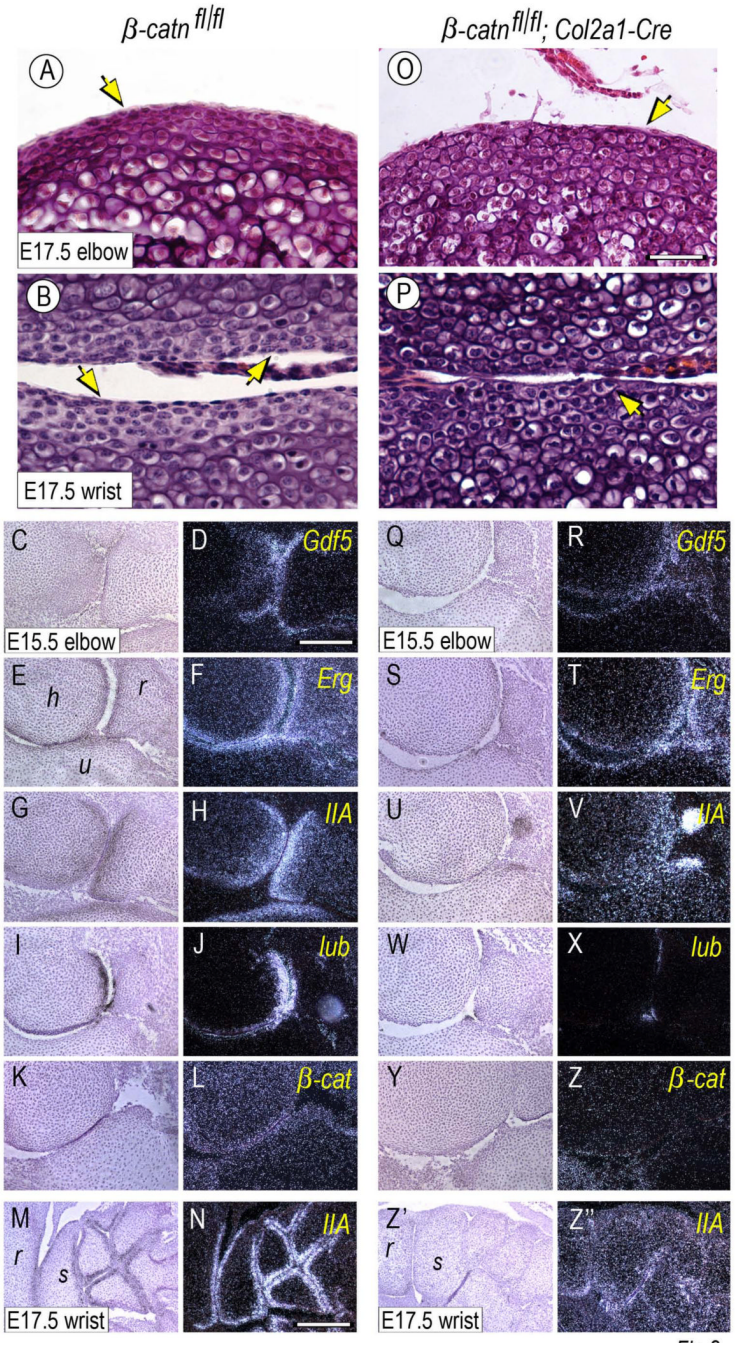

Fig. 8.

Superficial flat cell layer organization and gene expression patterns are defective in conditional *Col2a1-Cre β-catenin*-deficient joints. Elbow and wrist joints from E15.5 and E17.5 control (*β-catn* $^{fl/fl}$) and *β-catenin*-deficient (*β-catn* $^{fl/fl}$/*Col2a1-Cre*) mouse embryo littermates were processed for standard H&E histology and in situ hybridization. Mutant joints display an appreciable reduction in the high-density flat cell layers all along the joint surface (O-P, arrows) that are quite evident in control joints (A-B, arrows). (C-N) Control joints display characteristic, prominent and expected patterns of expression of joint markers including *Gdf5*, *Erg*, *collagen IIA* (*IIA*) and *lubricin* (*lub*) (D, F, H, J, N). There is also appreciable expression of endogenous *β-catenin* (*β-cat*) (L). (Q-Z") In contrast, mutant joints exhibit obvious decreases in gene

expression, particularly *collagen IIA* and *lubricin* (V, X, Z") and to a lesser extent *Gdf5* and *Erg* (R, T). Endogenous *β*-catenin expression was barely detectable (Z). Bar for A-B and O-P, 35 μm; bar for C-L and Q-Z, 150 μm; bar for M-N and Z'-Z", 250 μm.

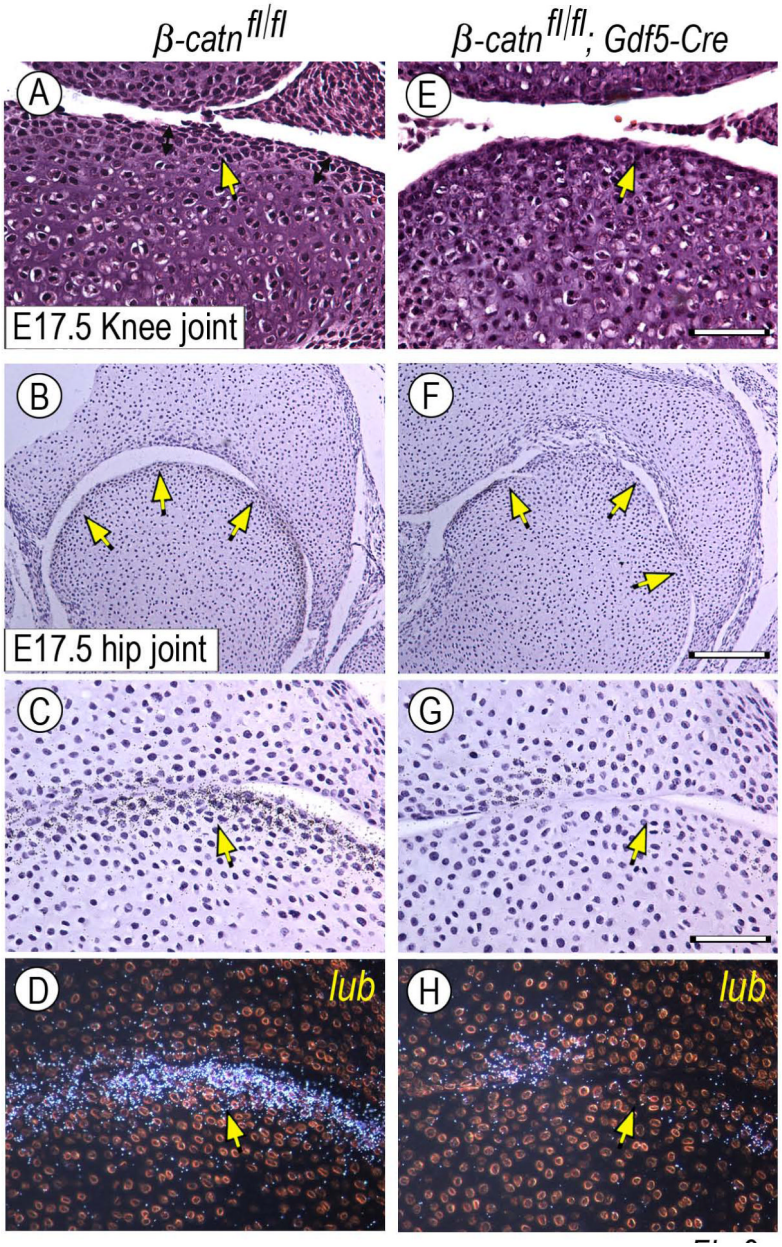

Fig. 9.

Defects in superficial flat cell layer and gene expression patterns in conditional *Gdf5-Cre β*-catenin-deficient joints. E17.5 knee and hip joints from control (*β-catn* $^{fl/fl}$) and *β*-catenin-deficient (*β-catn* $^{fl/fl}$/*Gdf5-Cre*) mouse embryo littermates were analyzed by standard histology and for expression of *lubricin*. (A-D) Control joints display the high cell density flat cell layers along the joint perimeter (A-C, arrows) and *lubricin* (*lub*) transcripts (D). (E-H) Instead, the superficial high-density layers are much less obvious in mutant joints (E-G, arrows) and *lubricin* expression is much reduced (H). Bar for A and E, 50 μm; bar for B and F, 175 μm; bar for C-D and G-H, 60 μm.

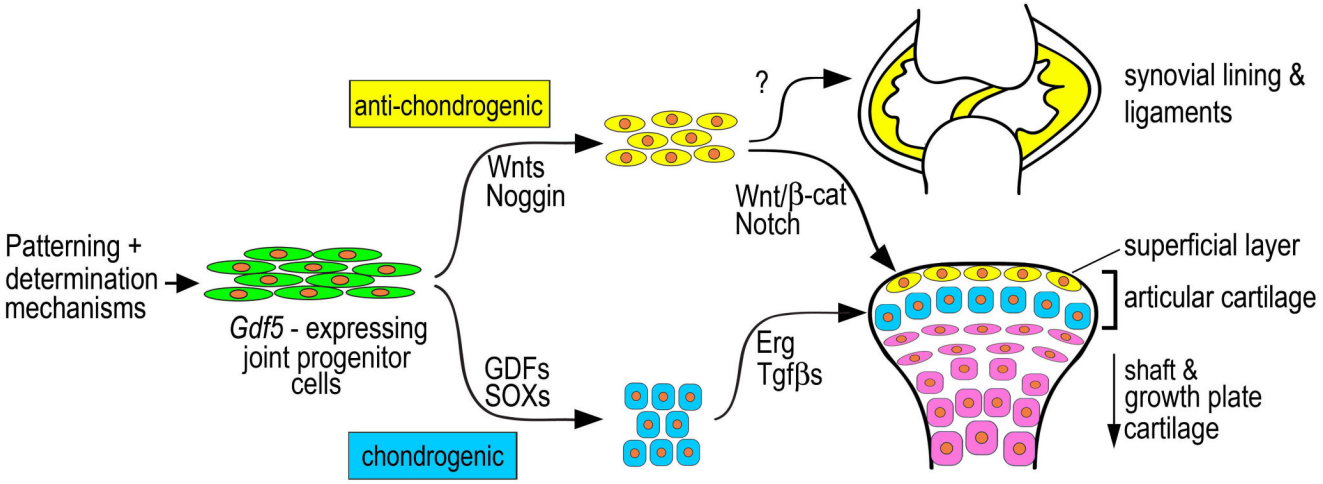

Fig 10.

Model of possible roles of *Gdf5*-expressing progenitor cells in joint formation and maintenance. Upstream patterning and determination mechanisms would initially induce emergence of the *Gdf5*-expressing cells at prospective limb joint sites. Spatio-temporally restricted action by members of *Gdf*, *Bmp* and *Sox* gene families would commit some of the cells to the chondrogenic lineage, and subsequent action by factors such as *Erg* (Iwamoto et al., 2007) and TGF*β* (Serra et al., 1997; Spagnoli et al., 2007) would promote formation of the bulk of articular cartilage. Anti-chondrogenic factors including Wnt/*β*-catenin and Notch signaling and BMP inhibitors such as Noggin would instead direct some of the cells toward fibrogenic and mesodermal lineages, resulting in formation of synovial lining, intra-joint ligaments, inner capsule and articular cartilage's superficial layer. The superficial layer would be maintained through life to serve as a source of lubricating molecules and as a possible source/recruiter of progenitor cells. Genes delineating the model above are not meant to be comprehensive.

Table 1

Quantification of alcian blue staining

	Treatment			
	None	**Gdf5**	**Noggin**	**PTHrP**
Control cultures	100 ± 1.2	140 ± 6.8**	61 ± 10.3**	113 ± 8.8
Wnt9a-cultures	78 ± 0.3*	109 ± 1.7	21 ± 2.4*	61 ± 2.3*

Images of control (uninfected) and *Wnt9a*-RCAS infected multiwell cultures stained with alcian blue shown in Fig. 6J and from two additional independent experiments were captured and analyzed by Image J software. Values are expressed relative to control untreated cultures (None) and represent averages and standard deviation.

* $p<0.01$ compared with cultures treated with the same factor,

** $p<0.01$ compared with control untreated cultures.